ARTICLE OPEN

Check for updates

Entanglement-interference complementarity and experimental demonstration in a superconducting circuit

Xin-Jie Huang[1,6], Pei-Rong Han[1,6], Wen Ning[1], Shou-Bang Yang[1], Xin Zhu[1], Jia-Hao Lü[1], Ri-Hua Zheng[1], Hekang Li[2], Zhen-Biao Yang[1]✉, Kai Xu[2,3], Chui-Ping Yang[4]✉, Qi-Cheng Wu[5], Dongning Zheng[2,3], Heng Fan[2,3] and Shi-Biao Zheng[1]✉

Quantum entanglement between an interfering particle and a detector for acquiring the which-path information plays a central role for enforcing Bohr's complementarity principle. However, the quantitative relation between this entanglement and the fringe visibility remains untouched upon for an initial mixed state. Here we find an equality for quantifying this relation. Our equality characterizes how well the interference pattern can be preserved when an interfering particle, initially carrying a definite amount of coherence, is entangled, to a certain degree, with a which-path detector. This equality provides a connection between entanglement and interference in the unified framework of coherence, revealing the quantitative entanglement-interference complementarity. We experimentally demonstrate this relation with a superconducting circuit, where a resonator serves as a which-path detector for an interfering qubit. The measured fringe visibility of the qubit's Ramsey signal and the qubit-resonator entanglement exhibit a complementary relation, in well agreement with the theoretical prediction.

npj Quantum Information (2023)9:43 ; https://doi.org/10.1038/s41534-023-00714-8

INTRODUCTION

Quantum coherence not only represents one of the most striking features of quantum mechanics, but also serves as a resource for quantum information processing[1–3]. A quantum mechanical object can simultaneously follow different paths in either ordinary space or in Hilbert space spanned by state vectors. Interference occurs when these paths are recombined and no path information is available. It is impossible to obtain the particle's path information without at the same time destroying the coherence between the paths and the resulting interference pattern; that is, any effort to determine which path the particle takes would involve coupling the particle to the which-path detector (WPD) and hence correlate their states. In the recoiling-slit gedanken experiment introduced by Einstein and Bohr[4], though the loss of the interference pattern is usually attributed to the position-momentum uncertainty relation, it can also be explained in terms of the entanglement between the photon and the two-slit apparatus induced by the path-dependent recoil[5]. In the gedanken experiment proposed by Scully et al.[6,7], where two high-quality micromaser cavities, each on one path of an atomic beam passing through a two-slit assembly, act as the WPD, the atomic path is marked by the photon the atom deposits in the corresponding cavity. In this case, the loss of the interference pattern of the atoms has no relation with the position-momentum uncertainty relation; instead, the entanglement between the atomic path and the photonic state of two cavities leads to the loss of the quantum coherence between the atomic paths, and hence destroys the interference. The disappearance of interference due to the introduction of a WPD has been demonstrated in different experiments[5–15], which cannot be explained by Heisenberg's uncertainty relation in any form.

In contrast to the case that the WPD states correlated with the two paths of the interfering particles are completely distinguishable, the duality relation is much more subtle in the intermediate regime[16–18], where only partial which-path information is available, so that the coherence between the paths is not completely lost and interference fringes with a reduced visibility are retained. In ref. [18], Englert performed a detailed analysis on this case by introducing a WPD, whose states associated with the interfering paths are not orthogonal. He showed that, for a given amount of which-path information stored in the WPD, quantified by the distinguishability, D, the fringe visibility, V, is limited by an inequality $D^2 + V^2 \leq 1$, which corresponds to a quantitative description of the wave-particle duality. For an imbalanced two-way interferometer without WPD, the inequality becomes $P^2 + V^2 \leq 1$, where P represents the path predictability. Recently, Bagan et al. generalized this result to the case with multiple interfering paths, deriving the relation between the coherence among these paths and the amount of path information[19]. The reduction of fringe visibility due to a partial acquisition of which-path information has been observed in the optical system[20], cavity QED[5,21], and superconducting circuit platform[15]. In the atomic interference experiment reported in Ref. [11], where the internal degree of freedom of an atom acts as the WPD for its spatial paths, the relation for the path information and fringe visibility was verified in the intermediate regime. In this experimental demonstration, the system-WPD entanglement plays a critical role for enforcing the complementarity principle, though it was not quantified in the experiment.

In recent years, the quantitative triality relation among the visibility, predictability, and entanglement was detailedly investigated in composite systems that are in a pure state[22–30], and was confirmed in classical optical interference experiments[31,32], as well as in single-photon experiments[33,34]. An experimental investigation involving two entangled superconducting qubits has also been reported[35], but where no interference experiment was

[1]Fujian Key Laboratory of Quantum Information and Quantum Optics, College of Physics and Information Engineering, Fuzhou University, Fuzhou, Fujian 350108, China. [2]Institute of Physics, Chinese Academy of Sciences, Beijing 100190, China. [3]CAS Center for Excellence in Topological Quantum Computation, Beijing 100190, China. [4]School of Physics, Hangzhou Normal University, Hangzhou 311121, China. [5]Quantum Information Research Center, Shangrao Normal University, Shangrao 334001, China. [6]These authors contributed equally: Xin-Jie Huang, Pei-Rong Han. ✉email: zbyang@fzu.edu.cn; yangcp@hznu.edu.cn; t96034@fzu.edu.cn

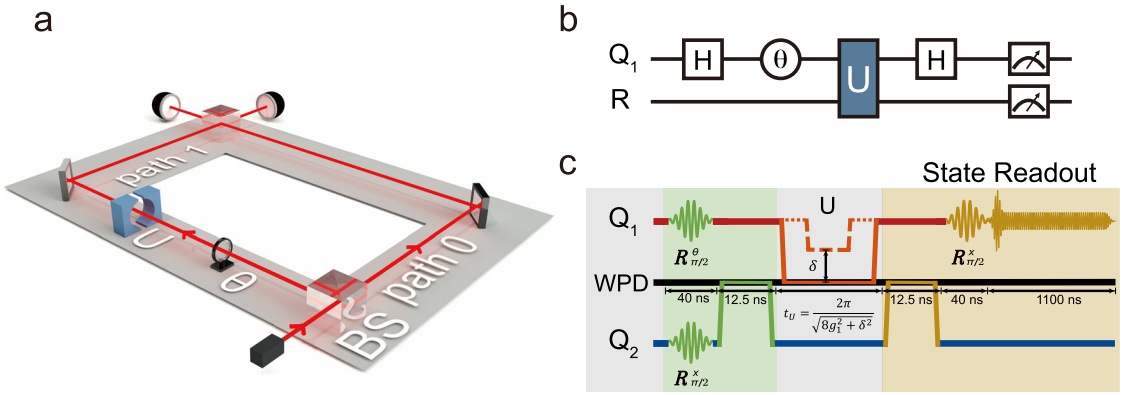

Fig. 1 Interferometer and pulse sequence. a Diagram of the two-way interferometer supplemented by a WPD. A quantum system is evolved to a superposition of taking paths 0 and 1 by the first beam-splitter (BS). Then it is subjected to an adjustable relative phase shift (θ), and coupled to the WPD which undergoes a unitary transformation, U, conditional on the system's path 1. After recombination of the two paths by the second BS, the system is detected. **b** Logic diagram of the on-chip Ramsey interferometer. A superconducting Xmon qubit, Q_1, acts as the interfering qubit, whose quantum state is split and recombined by two Hadamard transformations (H), in between which the which-path information in the quantum state space is controllably encoded on the photonic field of a resonator, R. A second Xmon qubit Q_2 is used for preparing and detecting the state of the resonator. **c** Pulse sequence. The interference experiment with which-path information acquisition consists of three parts: Preparation of the resonator's initial state $|W_0\rangle$ with Q_2; Ramsey interference supplemented with the WPD, realized by sandwiching the Q_1-resonator interaction between two $\pi/2$ pulses, $R^{\theta}_{\pi/2}$ and $R^{x}_{\pi/2}$; State readout.

performed. Here we investigate the relation among the fringe visibility of an interfering qubit, its quantum entanglement with a WPD, and the original coherence. We show that the system-WPD entanglement measured by concurrence and the available fringe visibility obey the equality $E^2 + V^2 = C_0^2$, where C_0 is the original coherence of the interfering system, which serves as a resource for producing entanglement and interference pattern. Our equality quantitatively characterizes the entanglement-interference complementarity in terms of the resource theory of coherence, in contrast with previous investigations. Due to the inevitable environmentally induced decoherence effects, it is experimentally challenging to prepare a real quantum system in a perfect pure state, so that investigation of a duality relation with a non-unity coherence resource is of experimental relevance. We experimentally investigate this relation with a superconducting Ramsey interferometer, where a resonator serves as the WPD for a qubit in its quantum state space. The entanglement between the WPD and the qubit is controlled via their effective interaction time, achieved by the qubit's frequency tunability. The values of C_0 and V are measured independently, with the experimental results well agreeing with theoretical predictions and revealing that coherence serves as a resource for both entanglement and interference. Unlike the photonic experiments[33,34], the present interference experiment is performed in a deterministic way, which pushes forward the experimental exploration of the entanglement-interference complementarity.

RESULTS

Theoretical predictions

Let us illustrate the underlying physics with a Mach-Zehnder interferometer, with the diagram shown in Fig. 1a, where the interfering system, initially traveling along path 0, passes through a beam-splitter (BS) which splits the path 0 into two paths 0 and 1. When traveling along path 1, the system is subsequently subjected to a phase shift θ and coupled to a WPD, which undergoes a unitary transformation, denoted as U. The second BS recombines the two paths. It is convenient to denote these two paths as the basis states $|0\rangle$ and $|1\rangle$, respectively. With this notation, the system can be described as a qubit, and the effect of each BS corresponds to the Hadamard transformation $\{|0\rangle \to (|0\rangle - \mathrm{i}|1\rangle)/\sqrt{2}; |1\rangle \to (|1\rangle - \mathrm{i}|0\rangle)/\sqrt{2}\}$. When the WPD is initially in a pure state $|W_0\rangle$, the qubit-WPD state after their coupling is

$$|\psi\rangle = \frac{1}{\sqrt{2}}\left(|0\rangle|W_0\rangle - \mathrm{i}e^{\mathrm{i}\theta}|1\rangle U|W_0\rangle\right). \tag{1}$$

After the second Hadamard transformation, the probability of detecting the qubit in the state $|1\rangle$ is

$$P_1 = \frac{1}{2}[1 + V_0\cos(\theta + \phi)], \tag{2}$$

where $V_0 = |\langle W_0|U|W_0\rangle|$ and $\phi = \arg(\langle W_0|U|W_0\rangle)$. This θ-dependent probability manifests the interference behavior, with the fringe visibility reduced to V_0 due to the qubit-WPD entanglement. When the WPD lies in a multi-dimensional Hilbert space, we map it to the two-dimensional space $\{|W_0\rangle, |W_1\rangle\}$ so that the qubit-WPD entanglement can be measured with concurrence[36], where

$$|W_1\rangle = \sqrt{\frac{1}{1 - V_0^2}}\left(U|W_0\rangle - V_0 e^{\mathrm{i}\phi}|W_0\rangle\right) \tag{3}$$

is orthogonal to $|W_0\rangle$. With this mapping, the joint qubit-WPD state can be considered as a two-qubit entangled state. The concurrence for measuring the amount of the qubit-WPD entanglement is $E = \sqrt{1 - V_0^2}$. This concurrence is equivalent to the distinguishability, D, which measures the path information stored in the WPD, and is defined as

$$D = \frac{1}{2}\mathrm{Tr}_{\mathrm{w}}\left|\rho_{\mathrm{w},0} - \rho_{\mathrm{w},1}\right|, \tag{4}$$

where $\rho_{\mathrm{w},0} = \langle 0|\rho|0\rangle/\mathrm{tr}_{\mathrm{w}}(\langle 0|\rho|0\rangle)$ and $\rho_{\mathrm{w},1} = \langle 1|\rho|1\rangle/\mathrm{tr}_{\mathrm{w}}(\langle 1|\rho|1\rangle)$ respectively denote the density operators of the WPD associated with the interfering qubit's $|0\rangle$ and $|1\rangle$ states after their coupling, with $\rho = |\psi\rangle\langle\psi|$ denoting the density operator for the joint qubit-WPD state, and the tracing is over the WPD's degree of freedom.

We note that $E = D$ holds only when the two paths of the interfering system are completely coherent. When the coherence between the two paths is partially lost before the qubit-WPD coupling, the corresponding qubit's state is described by the density operator

$$\rho_{\mathrm{q},0} = \frac{1}{2}\left[|0\rangle\langle 0| + |1\rangle\langle 1| + \mathrm{i}C_0\left(e^{-\mathrm{i}\theta}|0\rangle\langle 1| - e^{\mathrm{i}\theta}|1\rangle\langle 0|\right)\right], \tag{5}$$

Table 1. Experimental parameters.

Parameters	Q_1	Q_2
$\omega_j/2\pi$	5.967 GHz	5.354 GHz
$g_j/2\pi$	19.2 MHz	19.9 MHz
$T_{1,j}$	17.1 μs	23.4 μs
$T_{\varphi,j}$	3.6 μs	2.7 μs

$\omega_j/2\pi$: Q_j's idle frequency; g_j: Q_j-R coupling strength; $T_{1,j}$: Q_j's energy relaxation time; $T_{\varphi,j}$: Q_j's pure dephasing time. The other parameters can be found in the Supplementary Table 1.

where C_0 is the coherence between the two paths, defined as the sum of the moduli of the off-diagonal elements[1].

After the qubit-resonator coupling and the subsequent Hadamard transformation, the probability of detecting the qubit in the state $|1\rangle$ is

$$P_1' = \frac{1}{2}[1 + V\cos(\theta + \phi)], \tag{6}$$

where $V = C_0V_0$ is the fringe visibility. This visibility and the qubit-WPD entanglement satisfy the equality (see Supplementary Note 2)

$$E^2 + V^2 = C_0^2. \tag{7}$$

This implies that both the qubit-WPD concurrence and the fringe visibility are reduced by a factor of C_0 due to the decoherence between the paths before the qubit-WPD coupling. In distinct contrast, the distinguishability, $D = \sqrt{1 - V_0^2}$, is not affected by the decoherence, and consequently, $D^2 + V^2 > C_0^2$ unless $C_0 = 1$. The results can be interpreted as follows. The conditional unitary evolution arising from the qubit-WPD coupling corresponds to an incoherent operation, which cannot produce entanglement when the qubit is in an incoherent state before this operation[3]. Both the interference and the qubit-WPD entanglement originate from the original coherence of the interfering qubit; this coherence, as a resource, can be either converted to entanglement or used for interference. For a given coherence resource, the more the amount of entanglement, the weaker the interference effect. In contrast, the distinguishability does not depend on the coherence resource; instead, it is determined by the distance between the WPD states associated with the two paths. For example, even for $C_0 = 0$, D can reach 1 as long as the two WPD states are orthogonal. The equality of Eq. (7) also holds for the unbalanced interferometer, where the two paths are not equally populated before coupling to the WPD (see Supplementary Note 1). We note that this equality represents a more general triality relation, which reduces to the previously proposed triality equality[22–30] when the interfering qubit is initially a pure state so that $C_0^2 = 1 - P^2$, where P denotes the predictability.

Device and experimental scheme

These theoretical predictions can be demonstrated on different platforms with controlled natural or artificial atoms[37,38], among which circuit quantum electrodynamics systems represent a typical example owing to the available strong coupling between superconducting qubits and microwave photons[39,40]. The experiment is implemented with a circuit Ramsey interferometer, with the logic diagram of the process sketched in Fig. 1b. The device involves 5 frequency-tunable Xmon qubits[41–44], one of which (Q_1) acts as the interfering qubit, whose two lowest levels, denoted as $|0\rangle$ and $|1\rangle$, correspond to two interfering paths in the Hilbert space. Such a Ramsey interferometer is analogous to the Mach-Zehnder interferometer, where the BSs are replaced by two Hadamard transformations (H). The photonic field stored in a bus resonator, R, is used to acquire the which-path information of Q_1 before the recombination of the two interfering paths. A second qubit Q_2 serves as the ancilla for preparing and reading out the state of the resonator. In our experiment, the tunable phase shift θ between the two interfering paths is incorporated into the first microwave pulse. The experimental parameters are detailed in Table 1.

To enable the resonator to act as the WPD, before coupling to Q_1 it is prepared in the coherent superposition containing 0 and 1 photon: $|W_0\rangle = (|0_r\rangle - |1_r\rangle)/\sqrt{2}$. The resonator's conditional unitary evolution, U, is realized by tuning the frequency associated with Q_1's transition $|1\rangle \leftrightarrow |2\rangle$, ω_{12}, close to the resonator's frequency, where $|2\rangle$ represents the second excited state of Q_1. After an interaction time $\tau = \pi/\Omega$, the resonator undergoes an evolution, $U = e^{i\beta|1_r\rangle\langle 1_r|}$, conditional on Q_1's state $|1\rangle$, where $\beta = \pi[1 - \delta/(2\Omega)]$, with $\Omega = \sqrt{2g_1^2 + \delta^2}/4$ and $\delta = \omega_{12} - \omega_r$[45,46]. This conditional dynamics correlates the two paths (the qubit being in $|0\rangle$ or $|1\rangle$) produced by the first $\pi/2$ pulse ($R^{\theta}_{\pi/2}$) with the resonator's states $|W_0\rangle$ and $U|W_0\rangle$, respectively. After the second $\pi/2$ pulse $R^{x}_{\pi/2}$, the probability of detecting the qubit in $|1\rangle$ state is given by Eq. (2), which corresponds to a θ-dependent Ramsey interference signal, with the fringe visibility $V_0 = \cos(\beta/2)$.

Measurement of the entanglement-interference relation for a unity source coherence

The interference experiment starts by simultaneously driving the ancilla qubit Q_2 from the ground state $|0_a\rangle$ to the superposition state $(|0_a\rangle - i|1_a\rangle)/\sqrt{2}$ with a $\pi/2$ pulse $R^{x}_{\pi/2}$, and applying a $\pi/2$ pulse $R^{\theta}_{\pi/2}$ to Q_1 (Fig. 1c), which produces a $\pi/2$ rotation around the axis with an angle θ to x-axis on the equatorial plane of the Bloch sphere. Then Q_2 is tuned on-resonance with the resonator initially in the vacuum state $|0_r\rangle$ for a time 12.5 ns, which realizes a swapping operation, mapping the ancilla state to the resonator, preparing it in the superposition of the zero- and one-photon states required for storing the which-path information of the interfering qubit. After preparation of the WPD's state $|W_0\rangle$, Q_2 is biased back to its idle frequency. Subsequently, Q_1's transition $|1\rangle \leftrightarrow |2\rangle$ is tuned close to the resonator's frequency to realize the conditional evolution U, resulting in entanglement between Q_1 and the resonator. Following this conditional dynamics, Q_1 is tuned back to its idle frequency, where the second $\pi/2$ pulse $R^{x}_{\pi/2}$ is applied. The Ramsey signals, defined as the probability for measuring Q_1 in $|1\rangle$ state as a function of θ, for conditional phase shifts $\beta = \pi/4$, $\pi/2$, $3\pi/4$, and π are displayed in Fig. 2a, b, c, d, respectively. As expected, the fringe visibility decreases as β increases for $0 \le \beta \le \pi$, as a result of the increasing entanglement between Q_1 and the resonator. The extracted fringe visibility as a function of β is denoted by diamonds in Fig. 2e, which is in well agreement with the numerical simulation (blue dashed line). We note that the qubit has a slight probability of being populated in the $|2\rangle$-state after the conditional phase shift, as a consequence of experimental imperfections. In the experiment, the maximal residual population of this state is measured to be 0.022, which only changes the Ramsey fringe visibility by about 1.29%.

To quantitatively investigate the change of entanglement between Q_1 and the resonator accompanying the decrease of the fringe visibility, we map the state of the resonator back to Q_2 for joint state tomography. This is achieved by tuning Q_2 on resonance with the resonator for a time of 12.5 ns after the resonator's interaction with Q_1, and then biasing back it to its idle frequency. Then the joint Q_1-Q_2 density matrix is measured by quantum state tomography (see Supplementary Note 10). The resulting Q_1-Q_2 concurrence as a function of β is represented by dots in Fig. 2e, which agrees with the simulation (green dashed line). As expected, the higher the concurrence, the lower the fringe contrast. The source coherence C_0 is measured through quantum state tomography on Q_1 right after the first $\pi/2$ pulse

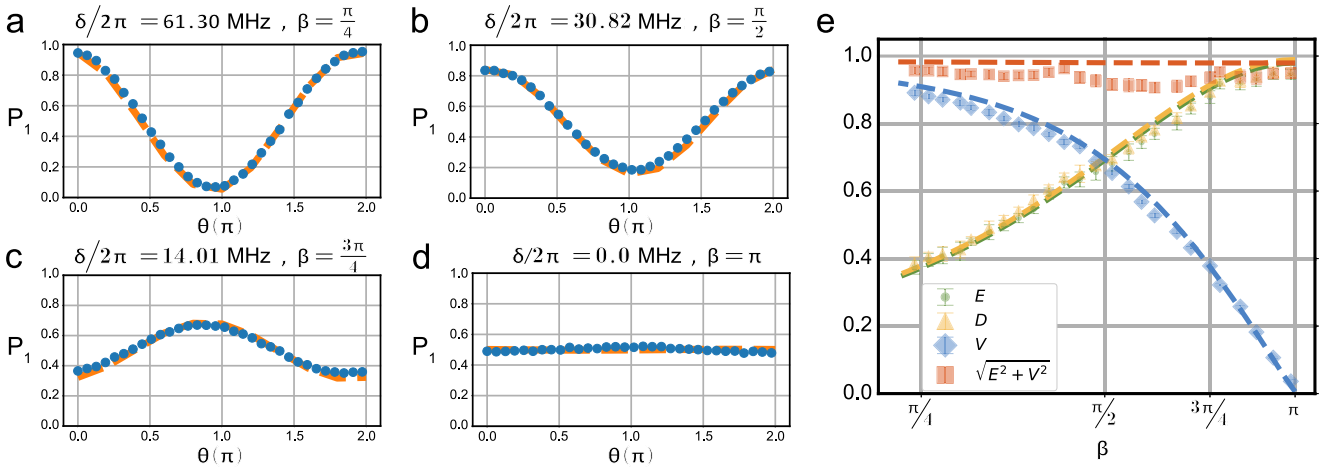

Fig. 2 Measured entanglement-interference relation for a unity source coherence. The Ramsey interference is revealed by the probability of measuring the test qubit in the state $|1\rangle$ as a function of θ for different conditional phase shift β: **a** $\pi/4$; **b** $\pi/2$; **c** $3\pi/4$; **d** π. The corresponding fringes visibilities are 0.8853, 0.6473, 0.3184, and 0.0311, respectively. **e** Measured fringe visibility V (diamonds), Q_1-Q_2 concurrence E (dots), and distinguishability D (triangles) as a function of the conditional phase shift β of the resonator. E is measured after mapping the resonator's state back to Q_2. The results are obtained with the pulse sequences shown in the Supplementary Fig. 5. Squares denote the quantity $\sqrt{E^2+V^2}$. The dashed lines correspond to numerical results. The error bars are the standard deviation of the measurements. For some data points, the error bar is smaller than the marker.

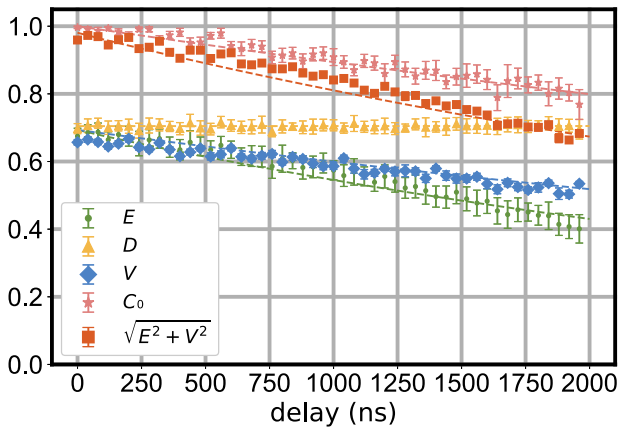

Fig. 3 Measured entanglement-interference relations for different source coherences. The diamonds, dots, stars, and triangles denote the fringe visibility, concurrence, source coherence, and distinguishability, respectively. The results are obtained with the preparation of the WPD's superposition state $|W_0\rangle$ delayed by a preset time. The conditional phase shift of the resonator induced by coupling to Q_1 is $\beta = \pi/2$. Squares denote evolution of the quantity $\sqrt{E^2+V^2}$. The error bars represent the standard deviation of the measurements. For some data points, the error bar is smaller than the corresponding symbol.

$R^{\theta}_{\pi/2}$; preparation of the WPD state $|W_0\rangle$, coupling Q_1 to the WPD, and subsequent WPD-Q_2 state mapping are unnecessary for measuring C_0. The quantity $\sqrt{E^2+V^2}$ as a function of β is also displayed in Fig. 2e (squares), which well coincides with the measured C_0. The slight difference between the measured values of these quantities mainly results from energy relaxation and dephasing of the qubits and photon loss of the resonator.

We further reveal the relation between the distinguishability of the two paths and the entanglement between the interfering qubit and the WPD for the fully coherent qubit state. This is achieved by extracting the density matrices $\rho_{w,0}$ and $\rho_{w,1}$ of the WPD associated with the interfering qubit's $|0\rangle$ and $|1\rangle$ states after their coupling, obtained by projecting the measured Q_1-Q_2 density matrix ρ to Q_1's basis states $|0\rangle$ and $|1\rangle$, which are displayed in Supplementary Note 3. The resulting distinguishability D, as a function of the conditional phase β, is denoted by the triangles of Fig. 2e, which coincides with the Q_1-Q_2 concurrence (green dots) very well, verifying the WPD acquires the which-path information by entangling its state with the interfering qubit.

Measurement of entanglement-interference relations for different source coherences

To further confirm the quantitative relation among the system's original coherence C_0, fringe visibility V, and the system-WPD entanglement E for partially coherent qubit states, we adjust the temporal orders of the $\pi/2$ pulse ($R^{\theta}_{\pi/2}$) of the Ramsey interferometer and the preparation of the WPD's superposition state $|W_0\rangle$, and delay this preparation procedure for a time t after $R^{\theta}_{\pi/2}$. Due to the energy relaxation and dephasing during this delay, the density operator of Q_1 is given by Eq. (5), with $C_0 \simeq e^{-t/2T_1 - t/T_\varphi}$. The conditional phase shift of the resonator induced by coupling to Q_1 is set to $\beta = \pi/2$. The measured fringe visibility V (diamonds), Q_1-Q_2 concurrence E (dots), the system's original coherence C_0 (stars), and the distinguishability D (triangles), as functions of the delay t, are displayed in Fig. 3. As expected, both V and E decrease as the delay increases. In addition to the decoherence of the test qubit, the concurrence is affected by thermal excitations of the ancilla and the resonator during the delay, which accounts for the result that the measured concurrence decays faster than the visibility, so that the measured $\sqrt{E^2+V^2}$ (squares) is smaller than C_0. On the other hand, measured D (triangles) almost does not change with the delay, which implies that it is independent of the source coherence.

DISCUSSION

We have derived an equality relating the fringe visibility of an interfering system and its entanglement with a WPD inside an interferometer to the original coherence. The result reveals, for a given amount of coherence resource, the available fringe visibility is

determined by the system-WPD entanglement: the stronger the system's entanglement with the WPD, the lower the available fringe visibility. We perform an experimental test of this relation in a superconducting circuit, in which a resonator is prepared in a superposition of zero- and one-photon states and acts as the WPD for a superconducting Xmon qubit. The measured results agree well with the theoretical predictions, confirming the entanglement-interference complementarity.

DATA AVAILABILITY

All data needed to evaluate the conclusions in the paper are present in the paper and/or the Supplementary Materials. Additional data related to this paper may be requested from the authors.

Received: 8 October 2022; Accepted: 17 April 2023;
Published online: 02 May 2023

REFERENCES

1. Baumgratz, T., Cramer, M. & Plenio, M. B. Quantifying coherence. *Phys. Rev. Lett.* **113**, 140401 (2014).
2. Streltsov, A., Singh, U., Dhar, H. S., Bera, M. N. & Adesso, G. Measuring quantum coherence with entanglement. *Phys. Rev. Lett.* **115**, 020403 (2015).
3. Tan, K. C., Choi, S., Kwon, H. & Jeong, H. Coherence, Quantum Fisher information, superradiance, and entanglement as interconvertible resources. *Phys. Rev. A* **97**, 052304 (2018).
4. Bohr, N. *Quantum Theory and Measurement* (eds Wheeler, J. A. & Zurek, W. H.) 9–49 (Princeton University Press, Princeton, NJ, 1984).
5. Bertet, P. et al. A complementarity experiment with an interferometer at the quantum-classical boundary. *Nature* **411**, 166–170 (2001).
6. Scully, M. O., Englert, B.-G. & Walther, H. Quantum optical tests of complementarity. *Nature* **351**, 111–116 (1991).
7. Englert, B.-G., Walther, H. & Scully, M. O. Quantum optical ramsey fringes and complementarity. *Appl. Phys. B* **54**, 366–368 (1992).
8. Gerry, C. C. Complementarity and quantum erasure with dispersive atom-field interactions. *Phys. Rev. A* **53**, 1179–1182 (1996).
9. Zheng, S.-B. A simplified scheme for testing complementarity and realizing quantum eraser. *Opt. Commun.* **173**, 265–267 (2000).
10. Buks, E., Schuster, R., Heiblum, M., Mahalu, D. & Umansky, V. Dephasing in electron interference by a 'which-path' detector. *Nature* **391**, 871–874 (1998).
11. Dürr, S., Nonn, T. & Rempe, G. Origin of quantum-mechanical complementarity probed by a 'which-way' experiment in an atom interferometer. *Nature* **395**, 33–37 (1998).
12. Dürr, S., Nonn, T. & Rempe, G. Fringe visibility and which-way information in an atom interferometer. *Phys. Rev. Lett.* **81**, 5705–5709 (1998).
13. Herzog, T. J., Kwiat, P. G., Weinfurter, H. & Zeilinger, A. Complementarity and the quantum eraser. *Phys. Rev. Lett.* **75**, 3034–3037 (1995).
14. Kim, Y.-H., Yu, R., Kulik, S. P., Shih, Y. & Scully, M. O. Delayed "choice"quantum eraser. *Phys. Rev. Lett.* **84**, 1–5 (2000).
15. Liu, K. et al. A twofold quantum delayed-choice experiment in a superconducting circuit. *Sci. Adv.* **3**, e1603159 (2017).
16. Wootters, W. K. & Zurek, W. H. Complementarity in the double-slit experiment: quantum nonseparability and a quantitative statement of Bohr's principle. *Phys. Rev. D* **19**, 473–484 (1979).
17. Jaeger, G., Shimony, A. & Vaidman, L. Two interferometric complementarities. *Phys. Rev. A* **51**, 54–67 (1995).
18. Englert, B.-G. Fringe visibility and which-way information: an inequality. *Phys. Rev. Lett.* **77**, 2154–2157 (1996).
19. Bagan, E., Bergou, J. A., Cottrell, S. S. & Hillery, M. Relations between coherence and path information. *Phys. Rev. Lett.* **116**, 160406 (2016).
20. Zou, X. Y., Wang, L. J. & Mandel, L. Induced coherence and indistinguishability in optical interference. *Phys. Rev. Lett.* **67**, 318–321 (1991).
21. Brune, M. et al. Observing the progressive decoherence of the "meter" in a quantum measurement. *Phys. Rev. Lett.* **77**, 4887–4890 (1996).
22. Jakob, M. & Bergou, J. A. Complementarity and entanglement in bipartite qudit systems. *Phys. Rev. A* **76**, 052107 (2007).
23. Jakob, M. & Bergou, J. A. Quantitative complementarity relations in bipartite systems: entanglement as a physical reality. *Opt. Commun.* **283**, 827–830 (2010).
24. Qureshi, T. Predictability, distinguishability, and entanglement. *Opt. Lett.* **46**, 492–495 (2021).
25. Roy, A. K., Pathania, N., Chandra, N. K., Panigrahi, P. K. & Qureshi, T. Coherence, path predictability, and I concurrence: a triality. *Phys. Rev. A* **105**, 032209 (2022).
26. De Zela, F. Optical approach to concurrence and polarization. *Opt. Lett.* **43**, 2603–2606 (2018).
27. Qian, X.-F. & Agarwal, G. S. Quantum duality: a source point of view. *Phys. Rev. Res.* **2**, 012031(R) (2020).
28. Yoon, T. H. & Cho, M. Quantitative complementarity of wave-particle duality. *Sci. Adv.* **7**, eabi9268 (2021).
29. Basso, M. L. W. & Maziero, J. Entanglement monotones connect distinguishability and predictability. *Phys. Lett. A* **425**, 127875 (2021).
30. Qin, W., Miranowicz, A., Long, G., You, J. Q. & Nori, F. Proposal to test quantum wave-particle superposition on massive mechanical resonators. *npj Quantum Inf.* **5**, 58 (2019).
31. Qian, X.-F., Vamivakas, A. N. & Eberly, J. H. Entanglement limits duality and vice versa. *Optica* **5**, 942–947 (2018).
32. Norrman, A., Friberg, A. T. & Leuchs, G. Vector-light quantum complementarity and the degree of polarization. *Optica* **7**, 93–97 (2020).
33. Qian, X.-F. et al. Turning off quantum duality. *Phys. Rev. Res.* **2**, 012016(R) (2020).
34. Chen, D.-X. et al. Experimental investigation of wave-particle duality relations in asymmetric beam interference. *npj Quantum Inf.* **8**, 101 (2022).
35. Schwaller, N., Dupertuis, M. A. & Javerzac-Galy, C. Evidence of the quantum entanglement constraint on wave-particle duality using the IBM Q quantum computer. *Phys. Rev. A* **103**, 022409 (2021).
36. Wootters, W. K. Entanglement of formation of an arbitrary state of two qubits. *Phys. Rev. Lett.* **80**, 2245–2248 (1998).
37. Buluta, I., Ashhab, S. & Nori, F. Natural and artificial atoms for quantum computation. *Rep. Prog. Phys.* **74**, 104401 (2011).
38. Georgescu, I. M., Ashhab, S. & Nori, F. Quantum Simulation. *Rev. Mod. Phys.* **86**, 153–185 (2014).
39. You, J. Q. & Nori, F. Atomic physics and quantum optics using superconducting circuits. *Nature* **474**, 589–597 (2011).
40. Gu, X., Kockum, A. F., Miranowicz, A., Liu, Y.-X. & Nori, F. Microwave photonics with superconducting quantum circuits. *Phys. Rep.* **718-719**, 1–102 (2017).
41. Song, C. et al. Continuous-variable geometric phase and its manipulation for quantum computation in a superconducting circuit. *Nat. Commun.* **8**, 1061 (2017).
42. Ning, W. et al. Deterministic entanglement swapping in a superconducting circuit. *Phys. Rev. Lett.* **123**, 060502 (2019).
43. Yang, Z.-B. et al. Experimental demonstration of entanglement-enabled universal quantum cloning in a circuit. *npj Quantum Inf.* **7**, 44 (2021).
44. Xu, K. et al. Demonstration of a non-Abelian geometric controlled-NOT gate in a superconducting circuit. *Optica* **8**, 972–976 (2021).
45. Rauschenbeutel, A. et al. Coherent operation of a tunable quantum phase gate in cavity QED. *Phys. Rev. Lett.* **83**, 5166–5169 (1999).
46. Mariantoni, M. et al. Implementing the quantum von Neumann architecture with superconducting circuits. *Science* **334**, 61–65 (2011).

ACKNOWLEDGEMENTS

This work was supported by the National Natural Science Foundation of China (Grant No. 12274080, No. 11875108, No. 11934018, No. 92065114, No. T2121001, No. 12264040, and No. U21A20436), Innovation Program for Quantum Science and Technology (Grant No. 2021ZD0300200), the Strategic Priority Research Program of Chinese Academy of Sciences (Grant No. XDB28000000), the Key-Area Research and Development Program of Guangdong Province, China (Grant No. 2020B0303030001), Beijing Natural Science Foundation (Grant No. Z200009), and Project from Fuzhou University under (Grant No. JG202001-2, No. 049050011050).

AUTHOR CONTRIBUTIONS

S.-B.Z. derived the equality and conceived the experiment. X.-J.H. and P.-R.H. performed the experiment and analyzed the data, under supervision of Z.-B.Y. and S.-B.Z. S.-B.Z., Z.-B.Y., and C.-P.Y. cowrote the manuscript with feedbacks from all authors. All authors contributed to interpretation of the observed phenomena and helped to improve presentation of the manuscript.

COMPETING INTERESTS

The authors declare no competing interests.

ADDITIONAL INFORMATION

Supplementary information The online version contains supplementary material available at https://doi.org/10.1038/s41534-023-00714-8.

Correspondence and requests for materials should be addressed to Zhen-Biao Yang, Chui-Ping Yang or Shi-Biao Zheng.

Reprints and permission information is available at http://www.nature.com/reprints

Publisher's note Springer Nature remains neutral with regard to jurisdictional claims in published maps and institutional affiliations.